Journal of Nonlinear Modeling and Analysis
Volume 6, Number 4, December 2024, 890–918
http://jnma-online.com
DOI:10.12150/jnma.2024.890

Dynamics Analysis and Optimal Control for an Avian Influenza Model among Multi-Populations*

Yantao Luo[1,2†], Jianhua Huang[1], Xiao Wang[1†], Tingting Zheng[3] and Zhidong Teng[2]

Abstract In this paper, a compartment model is formulated to study the transmission dynamics of avian influenza virus among birds, poultry and human population. Due to the strong coupling of the system caused by the transmission route, there are some mathematical challenges to obtain the existence of the endemic equilibrium and its global asymptotic stability. Firstly, we give the well-posedness of the model and then discuss the threshold dynamics for three sub-models. Next, we give the threshold dynamics for the whole system: the disease-free equilibrium is locally asymptotically stable with $R_0 < 1$, and the other conditions are required for the global asymptotic stability of the disease-free equilibrium. The endemic-equilibrium is globally attractive when $R_0 > 1$. Furthermore, the sensitivity analysis and an optimal control problem are discussed. Finally, some numerical simulations are carried out to illustrate our theoretical results and visualize the impact of various parameters on model dynamics, which suggest that decreasing the recruitment rate and increasing the death rate of poultry, can only control the disease by simultaneously cutting off the transmission from birds to poultry and humans even if the ultimate scale of the disease can be effectively controlled. In addition, enhancing public awareness of prevention to reduce the transmission from birds and poultry to humans is also effective in controlling the final scale of disease.

Keywords Avian influenza, bird-poultry, coexistence equilibrium, existence and stability

MSC(2010) 92D30,34A34,92D25.

†the corresponding author.
Email address: luoyantaoxj@163.com (Y.Luo), jhhuang32@nudt.edu.cn (J.Huang), wxiao_98@nudt.edu.cn (X.Wang), ztt0711@163.com (T.Zheng) zhidong_teng@sina.com(Z.Teng)
[1]College of Science, National University of Defense Technology, Changsha, 410073, P.R. China
[2]College of Mathematics and Systems Science, Xinjiang University, Urumqi 830017, P.R. China
[3]College of Medical Engineering and Technology, Xinjiang Medical University, Urumqi 830017, P.R. China
*The authors were supported by the Natural Science Foundation of Xinjiang Uygur Autonomous Region (Grant Nos.2022D01C64 and 2022D01C699), the National Natural Science Foundation of China (Grant Nos.12201540),Natural Science Foundation of Human Province (Grant Nos.2022JJ30655).

1. Introduction

Avian influenza(AI) is an animal infection caused by an avian influenza virus (AIV), a type of influenza A virus, which normally does not infect humans [1]. However, since human infection with avian influenza (highly pathogenic A (H5N1)) was discovered in Hong Kong in 1997, the disease has become a zoonotic disease and has been of great concern to WHO worldwide [2]. From 2003 to July 14, 2023, 878 confirmed human cases of H5N1 virus infection have been reported to WHO including 458 deaths [3]. In addition, in the biological sense, there is a gap between the host types of different types of avian influenza viruses, and there are many subtypes of influenza viruses which can infect humans, such as, H1N1, H5N6, H7N9, and H9N2 [4], which belong to zoonotic virus AIV. The outbreak and epidemic of AI has had a serious impact on the aquaculture, catering, international trade and the ecological environment [5]. Therefore, it is necessary and meaningful to study influenza dynamics and design control strategies by understanding of the transmission mechanism of pathogenic AIV among birds, poultry and humans.

In recent years, it has been well-recognized that mathematical models are one of the most powerful tools for studying the dynamics of infectious disease because they can provide some useful epidemiological characteristics and effective prevention and control measures for relevant departments [6–10]. In particular, a number of sophisticated mathematical models for the spread of AI have been previously developed, see e.g. [11–20]. In particular, Liu et al. [19] introduced two different laws for the avian population into an AI bird-to-human model and analyzed their dynamical behavior. Bourouiba et al. [20] used the patch-type delay model to characterize the transmission mechanism migratory birds and non-migratory poultry, and further studied the role of migratory birds in the spread of H5N1 avian influenza. In addition, considering the effect of seasonal temperature and spatial heterogeneity environment on AI, Zheng et al. [14] proposed a time-spatial heterogeneity reaction-diffusion AI model. And Calvin et al. [12] formulated an avian–human influenza epidemic model with diffusion, nonlocal delay and spatial homogeneous environment to describe the transmission of avian influenza among poultry, humans and environment. However, there are many noises in the real world that affect the spread of diseases in different degrees [24,25]. Mate et al. [17] proposed a stochastic AI model with Ornstein–Uhlenbeck (O-U) process to investigate the relative contribution of direct and environmental transmission routes in the recurrence of AI epidemics. Zhou et al. [9] examined a stochastic avian influenza model with a nonlinear incidence rate within avian populations and the psychological effect within the human population, and they obtained the threshold dynamics of AI and the probability density function.

Although many avian influenza dynamics models, such as ODE, PDE, DDE, and SDE, have been discussed above, most of these models are only related to two compartments: birds and poultry, birds and humans. In fact, the spread of avian influenza often involves three groups: birds, poultry and humans. And the transmission path is also relatively complex, for example, wild birds and poultry can infect each other, and the wild birds can infect humans and even humans can be infected by poultry. Hence, it is meaningful and reasonable to incorporate the complex transmission routes among wild birds, poultry and humans. Nevertheless, it poses significant challenges to the dynamic analysis of the system, especially the existence and global stability of endemic equilibrium. In addition, although there

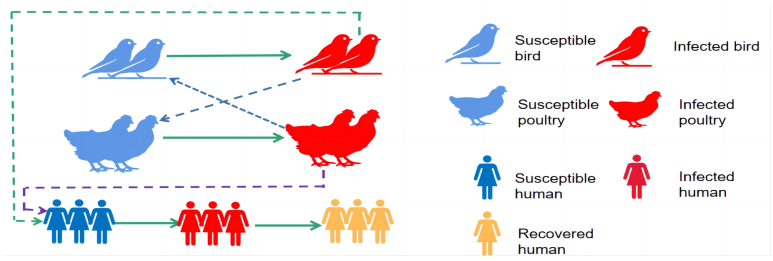

Figure 1. The diagram of the AI transmission

are few multi population dynamics models for avian influenza, there is some research on multi population dynamics models for other diseases, e.g., [21–23] and references therein, which can provide us with some reference for our analysis.

The organization of this paper is as follows. In Section 2, we establish the avian influenza model and introduce some preliminaries. In Section 3, the dynamic behavior of three sub-models are discussed, especially, the poultry-birds models. Sections 4 analyzes the dynamics of the whole system. The sensitivity analysis and an optimal control problem are discussed in Section 5. Section 6 carries out some numerical simulations to illustrate our theoretical results and visualize the impact of various parameters on model dynamics. A brief conclusion and discussion ends the paper.

2. Model formulation and preliminaries

To use mathematical models to characterize the dynamics of AI transmission between among birds, poultry and humans, we let $N_b(t)$, $N_p(t)$ and $N_h(t)$ represent the total population of birds, poultry and humans, respectively, at time t. In fact, populations infected with avian influenza have a higher mortality rate and generally do not recover. This is sufficient to divide the bird population under consideration into two classes: $S_b(t)$ and $I_b(t)$, representing the number of susceptible and infected birds at time t, respectively. And the poultry population is further divided as $S_p(t)$ and $I_p(t)$, which denote the number of susceptible and infected poultry at time t. For human population, we divide $N_h(t)$ into three classes: $S_h(t)$, $I_h(t)$ and $R_h(t)$, which respectively denote the number of susceptible, infected and recovered humans at time t. Based on the discussion above, we use the following diagram Fig.1 to illustrate the transmission mechanism among birds, poultry and humans, which gives rise to the following evolution model:

$$\begin{cases} \dfrac{\mathrm{d}S_b(t)}{\mathrm{d}t} =\Lambda_b - \beta_{bb}S_b(t)I_b(t) - \beta_{pb}S_b(t)I_p(t) - \mu_b S_b(t), \\ \dfrac{\mathrm{d}I_b(t)}{\mathrm{d}t} =\beta_{bb}S_b(t)I_b(t) + \beta_{pb}S_b(t)I_p(t) - (\mu_b + d_b)I_b(t), \\ \dfrac{\mathrm{d}S_p(t)}{\mathrm{d}t} =\Lambda_p - \beta_{pp}S_p(t)I_p(t) - \beta_{bp}S_p(t)I_b(t) - \mu_p S_p(t), \\ \dfrac{\mathrm{d}I_p(t)}{\mathrm{d}t} =\beta_{pp}S_p(t)I_p(t) + \beta_{bp}S_p(t)I_b(t) - (\mu_p + d_p)I_p(t), \\ \dfrac{\mathrm{d}S_h(t)}{\mathrm{d}t} =\Lambda_h - \beta_{bh}S_h(t)I_b(t) - \beta_{ph}S_h(t)I_p(t) - \mu_h S_h(t), \\ \dfrac{\mathrm{d}I_h(t)}{\mathrm{d}t} =\beta_{bh}S_h(t)I_b(t) + \beta_{ph}S_h(t)I_p(t) - (\gamma_h + \mu_h + d_h)I_h(t), \\ \dfrac{\mathrm{d}R_h(t)}{\mathrm{d}t} =\gamma_h I_h(t) - \mu_h R_h(t). \end{cases} \tag{2.1}$$

Here, $\Lambda_i (i = b, p, h)$ and $d_i (i = b, p, h)$ are the recruitment rate and the disease-induced death rate of bird/poultry/human population, respectively; $\mu_i (i = b, p)$ and μ_h are the death rate of bird/poultry(including natural death and culling) and the natural death rate of human, respectively; γ_h is the recover rate of human; β_{bb}, β_{pb}, β_{pp}, β_{bp}, β_{bh} and β_{ph} represent the transmission rate from bird to bird, from poultry to bird, from poultry to poultry, from bird to poultry, from bird to human and from poultry to human, respectively. Without loss of generality, we make the following assumptions:

(H1) All parameters used in model (2.1) are positive constants.

(H2) Duo to the more frequent contact between similar populations, the transmission rate between similar populations is greater than that between different populations, i.e., $\beta_{bb} \geq \beta_{pb}$ and $\beta_{pp} \geq \beta_{bp}$.

Before introducing the main results, based on practical biological significance, we first provide the following basic but necessary result for the solutions of model (2.1).

Theorem 2.1. *All solutions of model* (2.1) *are nonnegative and bounded if the initial conditions are nonnegative. Moreover,*

$$\Omega = \left\{ (S_b, I_b, S_p, I_p, S_h, I_h, R_h) \in \mathbb{R}^7_+ \ | 0 < N_b(t) \leq \frac{\Lambda_b}{\mu_b}, 0 < N_p(t) \leq \frac{\Lambda_p}{\mu_p}, \right.$$
$$\left. 0 < N_h(t) \leq \frac{\Lambda_h}{\mu_h} \right\},$$

is a positively invariant with respect to model (2.1).

Proof. Using the similar arguments as in [26, Theorem 3.1 and Theorem 3.2], we can easily complete this proof, so we omit it. □

3. Analysis of sub-model

In fact, humans are the ultimate host of avian influenza virus, which does not spread between humans or from humans to birds or poultry. From a mathematical

modeling perspective, it is evident that the fifth, sixth and seventh equations of model (2.1) can be decoupled. Hence, we are interested in studying the dynamics of the bird-only model, poultry-only model and bird-poultry model.

3.1. Bird/Poultry-only model

In this subsection, we analyze the dynamics of bird-only model and poultry-only model. Obviously, from model (2.1), it can be seen that when there are no birds or poultry, the model can degenerate into the following form

$$\begin{cases} \dfrac{\mathrm{d}S_i(t)}{\mathrm{d}t} =\Lambda_i - \beta_{ii}S_i(t)I_i(t) - \mu_i S_i(t), \\ \dfrac{\mathrm{d}I_i(t)}{\mathrm{d}t} =\beta_{ii}S_i(t)I_i(t) - (\mu_i + d_i)I_i(t), \end{cases} \tag{3.1}$$

where $i = b, p$ represents the bird-only model and poultry-only model, respectively. It is obviously that model (3.1) always has the disease-free equilibrium $e_0^i = (S_{i*}, 0)$, where $S_{i*} = \Lambda_i/\mu_i$. The basic reproduction number of model (3.1) is given by

$$\mathcal{R}_0^i = \frac{\Lambda_i \beta_{ii}}{\mu_i(\mu_i + d_i)},$$

which is defined as the average number of new infections generated by a single infected bird ($i = b$)/poultry($i = p$) in a completely susceptible population. In addition, by simple computation, there exists an endemic equilibrium for model (3.1) as follows,

$$e_1^i = \left(\frac{\mu_i + d_i}{\beta_{ii}}, \frac{\Lambda_i\beta_{ii} - \mu_i(\mu_i + d_i)}{\beta_{ii}(\mu_i + d_i)}\right),\ i = b, p,$$

which is only biologically meaningful for $\mathcal{R}_0^i \geq 1$, $i = b, p$. Furthermore, in terms of the threshold dynamics for model (3.1), we have the following result.

Theorem 3.1. *If $\mathcal{R}_0^i < 1$, then e_0^i is globally asymptotically stable; and if $\mathcal{R}_0^i > 1$, then e_1^i is globally asymptotically stable.*

Proof. The proof is the same as [6, Lemma 2] with $b = 0$, hence, we omit it. □

3.2. Bird-poultry model

As the main transmission host of avian influenza virus, the dynamics of birds and bird coupling models are crucial for the dynamic of the whole system. Hence, we mainly give the dynamics analysis for the following bird-poultry coupled model:

$$\begin{cases} \dfrac{\mathrm{d}S_b(t)}{\mathrm{d}t} =\Lambda_b - \beta_{bb}S_b(t)I_b(t) - \beta_{pb}S_b(t)I_p(t) - \mu_b S_b(t), \\ \dfrac{\mathrm{d}I_b(t)}{\mathrm{d}t} =\beta_{bb}S_b(t)I_b(t) + \beta_{pb}S_b(t)I_p(t) - (\mu_b + d_b)I_b(t), \\ \dfrac{\mathrm{d}S_p(t)}{\mathrm{d}t} =\Lambda_p - \beta_{pp}S_p(t)I_p(t) - \beta_{bp}S_p(t)I_b(t) - \mu_p S_p(t), \\ \dfrac{\mathrm{d}I_p(t)}{\mathrm{d}t} =\beta_{pp}S_p(t)I_p(t) + \beta_{bp}S_p(t)I_b(t) - (\mu_p + d_p)I_p(t). \end{cases} \tag{3.2}$$

From Theorem 2.1, we can similarly obtain that model (3.2) possesses the following positively invariant set

$$\Omega_{bp} = \left\{ (S_b, I_b, S_p, I_p) \in \mathbb{R}^4_+ \mid 0 < N_b(t) \leq \frac{\Lambda_b}{\mu_b}\ 0 < N_p(t) \leq \frac{\Lambda_p}{\mu_p} \right\}.$$

In addition, model (3.2) always has a disease-free equilibrium given by $E_0^{bp} = (S_{b*}, 0, S_{p*}, 0)$. Now, we use the next generation matrix method developed by [28, Lemma 1] to calculate the basic reproduction number for model (3.2). Let

$$F = \begin{pmatrix} \frac{\beta_{bb}\Lambda_b}{\mu_b} & \frac{\beta_{pb}\Lambda_b}{\mu_b} \\ \frac{\beta_{bp}\Lambda_p}{\mu_p} & \frac{\beta_{pp}\Lambda_p}{\mu_p} \end{pmatrix}, \qquad V = \begin{pmatrix} \mu_b + d_b & 0 \\ 0 & \mu_p + d_p \end{pmatrix}.$$

The basic reproduction number R_0 is defined to be the spectral radius (dominant eigenvalue) of the non-negative matrix FV^{-1}, denoted by $\rho(FV^{-1})$. Thus,

$$\mathcal{R}_0 = \frac{1}{2}\left[\mathcal{R}_0^b + \mathcal{R}_0^p + \sqrt{(\mathcal{R}_0^b - \mathcal{R}_0^p)^2 + 4\mathcal{R}_0^b\mathcal{R}_0^p \frac{\beta_{bp}\beta_{pb}}{\beta_{bb}\beta_{pp}}}\right].$$

Remark 3.1. According to the positivity of model parameters and the expression of $\mathcal{R}_0$, it is easy to obtain $\mathcal{R}_0 > \max\{\mathcal{R}_0^b, \mathcal{R}_0^p\}$. In fact, if $\beta_{bp} = 0$ or $\beta_{pb} = 0$, then $\mathcal{R}_0 = \max\{\mathcal{R}_0^b, \mathcal{R}_0^p\}$, which implies that poultry-to-bird and bird-to-poultry transmission increases the risk of infection.

When it comes to our greatest concern about the existence of endemic equilibrium for model (3.2), biologically speaking, the question is whether birds and poultry can coexist while infected with avian influenza in the absence of any control strategies. Denote $(\widetilde{S}_b^*, \widetilde{I}_b^*, \widetilde{S}_p^*, \widetilde{I}_p^*)$ as an arbitrary equilibrium of the bird-poultry model (3.2), which satisfies the following equations:

$$\begin{aligned} &\Lambda_b - \beta_{bb}\widetilde{S}_b^*\widetilde{I}_b^* - \beta_{pb}\widetilde{S}_b^*\widetilde{I}_p^* - \mu_b\widetilde{S}_b^* = 0, \qquad \beta_{bb}\widetilde{S}_b^*\widetilde{I}_b^* + \beta_{pb}\widetilde{S}_b^*\widetilde{I}_p^* - (\mu_b + d_b)\widetilde{I}_b^* = 0, \\ &\Lambda_p - \beta_{pp}\widetilde{S}_p^*\widetilde{I}_p^* - \beta_{bp}\widetilde{S}_p^*\widetilde{I}_b^* - \mu_p\widetilde{S}_p^* = 0, \qquad \beta_{pp}\widetilde{S}_p^*\widetilde{I}_p^* + \beta_{bp}\widetilde{S}_p^*\widetilde{I}_b^* - (\mu_p + d_p)\widetilde{I}_p^* = 0. \end{aligned} \tag{3.3}$$

From the first two equations of model (3.3), we have

$$\widetilde{I}_p^* = -\frac{\beta_{bb}}{\beta_{pb}}\widetilde{I}_b^* + \frac{\Lambda_b\mu_b}{\beta_{pb}}\frac{1}{\Lambda_b - (\mu_b + d_b)\widetilde{I}_b^*} - \frac{\mu_b}{\beta_{pb}}. \tag{3.4}$$

Further, by the last two equations of model (3.2), we can easily obtain

$$\widetilde{I}_b^* = -\frac{\beta_{pp}}{\beta_{bp}}\widetilde{I}_p^* + \frac{\Lambda_p\mu_p}{\beta_{bp}}\frac{1}{\Lambda_p - (\mu_p + d_p)\widetilde{I}_p^*} - \frac{\mu_p}{\beta_{bp}}. \tag{3.5}$$

For simplicity, let $(x, y) = (\widetilde{I}_b^*, \widetilde{I}_p^*)$. It follows from equations (3.4) and (3.5) that the following two curves:

$$\mathbf{C_1}: y = f(x) = -\frac{\beta_{bb}}{\beta_{pb}}x + \frac{\Lambda_b\mu_b}{\beta_{pb}}\frac{1}{\Lambda_b - (\mu_b + d_b)x} - \frac{\mu_b}{\beta_{pb}},$$

and

$$\mathbf{C_2}: x = g(y) = -\frac{\beta_{pp}}{\beta_{bp}}y + \frac{\Lambda_p\mu_p}{\beta_{bp}}\frac{1}{\Lambda_p - (\mu_p + d_p)y} - \frac{\mu_p}{\beta_{bp}}.$$

Obviously, seeking the endemic equilibrium of system (3.2) is transformed into finding the intersection point of curve C_1 and curve C_2 in the feasible region $[0, \frac{\Lambda_b}{\mu_b}) \times [0, \frac{\Lambda_p}{\mu_p})$. By calculation, curve C_1 intersects the X-axis at two points denoted by $O(0,0)$ and $A = (x_1, 0) = (\frac{\mu_b(\mathcal{R}_0^b - 1)}{\beta_{bb}}, 0)$, and the asymptote equations of curve C_1 are as follows,

$$L_{11} : y = -\frac{\beta_{bb}}{\beta_{pb}} x - \frac{\mu_b}{\beta_{pb}} \quad \text{and} \quad L_{12} : x = \frac{\Lambda_b}{\mu_b + d_b}.$$

Clearly, the asymptote L_{12} is not going to be the right of line $x = \Lambda_b/\mu_b$. Moveover, the slope of the tangent line of curve C_1 at the point $O(0,0)$ is $k_1 = \frac{\beta_{bb}(1-\mathcal{R}_0^b)}{\beta_{pb}\mathcal{R}_0^b}$. Similarly, curve C_2 intersects the $y-$axis at the two points denoted by $O(0,0)$ and $B = (0, y_1) = (0, \frac{\mu_p(\mathcal{R}_0^p - 1)}{\beta_{pp}})$, and the asymptote equations of curve C_2 are given by

$$L_{21} : y = -\frac{\beta_{bp}}{\beta_{pp}} x - \frac{\mu_p}{\beta_{pp}} \quad \text{and} \quad L_{22} : y = \frac{\Lambda_p}{\mu_p + d_p}.$$

Obviously, the asymptote L_{22} is not going to be higher than line $y = \Lambda_p/\mu_p$. Moreover, the slope of the tangent line of curve C_2 at the point $O(0,0)$ is $k_2 = \frac{\beta_{bp}\mathcal{R}_0^p}{\beta_{pp}(1-\mathcal{R}_0^p)}$. From the expression of curves C_1 and C_2, we obtain that

$$y'' = f''(x) = \frac{2\Lambda_b\mu_b(\mu_b + d_b)^2}{\beta_{pb}[\Lambda_b - (\mu_b + d_b)x]^3}, \quad x'' = g''(y) = \frac{2\Lambda_p\mu_p(\mu_p + d_p)^2}{\beta_{bp}[\Lambda_p - (\mu_p + d_p)y]^3}.$$

Furthermore, curve C_1 is concave for $x \in (-\infty, \frac{\Lambda_b}{\mu_b + d_b})$, while it is convex for $x \in (\frac{\Lambda_b}{\mu_b + d_b}, \infty)$; and curve C_2 is concave for $y \in (-\infty, \frac{\Lambda_p}{\mu_p + d_p})$, while it is convex for $y \in (\frac{\Lambda_p}{\mu_p + d_p}, \infty)$. Based on the above basic analysis, we can obtain the following facts:

$$y \to \infty, \text{as } x \to \left[\frac{\Lambda_b}{\mu_b + d_b}\right]^-; \qquad y \to -\infty, \text{as } x \to \left[\frac{\Lambda_b}{\mu_b + d_b}\right]^+ \text{and } x \to \infty;$$

and

$$x \to \infty, \text{as } y \to \left[\frac{\Lambda_p}{\mu_p + d_p}\right]^-; \qquad x \to -\infty, \text{as } y \to \left[\frac{\Lambda_p}{\mu_p + d_p}\right]^+ \text{and } y \to \infty.$$

It can be concluded from the above analysis that curve C_1 only has at most two points of intersection with the X-axis and curve C_2 only has at most two points of intersection with the Y-axis. Considering other basic characteristics of these two curves (limit, concavity, asymptote), they have at most one positive intersection point, and they can only intersect within the space $\left(0, \frac{\Lambda_b}{\mu_b + d_b}\right) \times \left(0, \frac{\Lambda_p}{\mu_p + d_p}\right)$.

It is easily to verify that curves C_1 and C_2 always have an intersection $O(0,0)$. It corresponds to the disease-free equilibrium of system (3.2). Moreover, based on the above discussion, the existence of endemic equilibria for system (3.2) in Ω_{bp} can be divided into the following six cases:

$$(i) : \mathcal{R}_0^b > 1, \mathcal{R}_0^p > 1; \qquad (ii) : \mathcal{R}_0^b < 1, \mathcal{R}_0^p < 1; \qquad (iii) : \mathcal{R}_0^b \le 1, \mathcal{R}_0^p > 1;$$
$$(iv) : \mathcal{R}_0^b > 1, \mathcal{R}_0^p \le 1; \qquad (v) : \mathcal{R}_0^b = 1, \mathcal{R}_0^p < 1; \qquad (vi) : \mathcal{R}_0^b \le 1, \mathcal{R}_0^p = 1.$$

For case (i): $\mathcal{R}_0^b > 1, \mathcal{R}_0^p > 1$. In this case, $x_1 = \mu_b(\mathcal{R}_0^b - 1)/\beta_{bb}$ and $y_1 = \mu_p(\mathcal{R}_0^p - 1)/\beta_{pp}$ are positive. And curves C_1 and C_2 exist a unique positive intersection in Ω_{bp}, as shown in Fig.2 (c). Hence, model (3.2) exists a unique coexistence equilibrium denoted by E_+^{bp}.

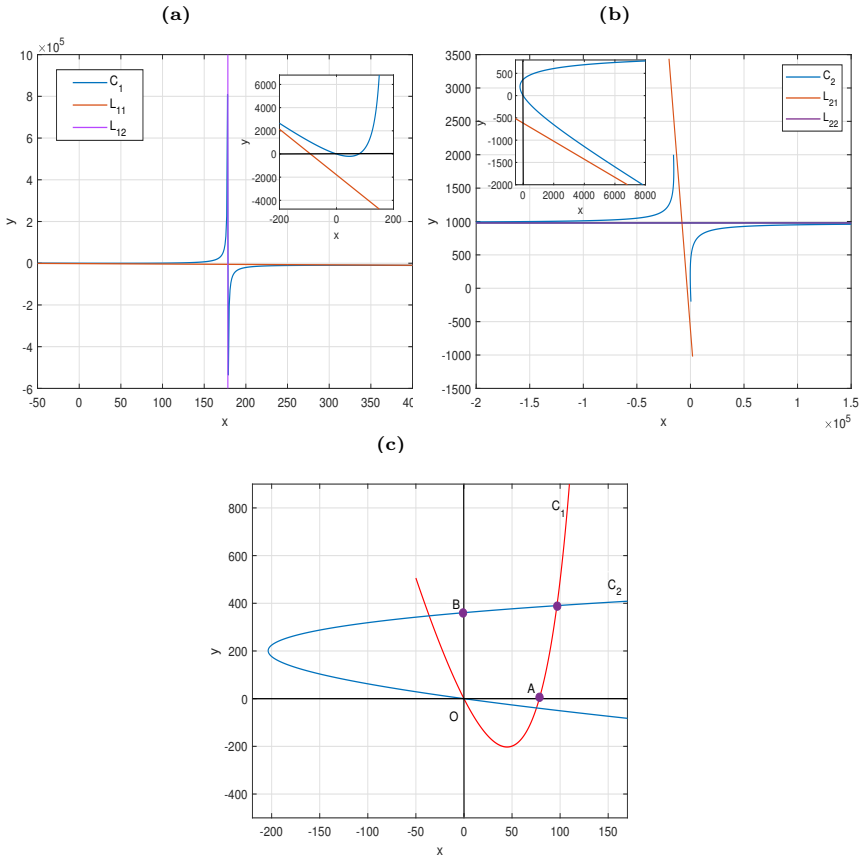

Figure 2. The intersections of curve C_1 and C_2 when $\mathcal{R}_0^b > 1$ and $\mathcal{R}_0^p > 1$.

For case (ii): $\mathcal{R}_0^b < 1$ and $\mathcal{R}_0^p < 1$. Obviously, x_1 and y_1 are negative. In this case, whether curves C_1 and C_2 intersect depends on the slope of the tangent line at the origin $O(0,0)$. From the expressions of k_1, k_2 and the basic reproduction number $\mathcal{R}_0$, we obtain that $k_1 > 0, k_2 > 0$, and

$$\frac{k_1}{k_2} = \frac{\beta_{bb}\beta_{pp}(1-\mathcal{R}_0^b)(1-\mathcal{R}_0^p)}{\beta_{bp}\beta_{pb}\mathcal{R}_0^b\mathcal{R}_0^p}.$$

In addition, we have

$$\mathcal{R}_0 > 1 \Leftrightarrow \sqrt{(\mathcal{R}_0^b - \mathcal{R}_0^p)^2 + 4\mathcal{R}_0^b\mathcal{R}_0^p\frac{\beta_{bp}\beta_{pb}}{\beta_{bb}\beta_{pp}}} > 2 - (\mathcal{R}_0^b + \mathcal{R}_0^p) > 0$$

$$\Leftrightarrow \mathcal{R}_0^b\mathcal{R}_0^p\frac{\beta_{bp}\beta_{pb}}{\beta_{bb}\beta_{pp}} > 1 - \mathcal{R}_0^b - \mathcal{R}_0^p + \mathcal{R}_0^b\mathcal{R}_0^p \Leftrightarrow \frac{\beta_{bb}\beta_{pp}(1-\mathcal{R}_0^b)(1-\mathcal{R}_0^p)}{\beta_{bp}\beta_{pb}\mathcal{R}_0^b\mathcal{R}_0^p} < 1.$$

Hence, $\mathcal{R}_0 > 1$ if and only if $k_1 < k_2$ and $\mathcal{R}_0 \leq 1$ if and only if $k_1 \leq k_2$. With the help of computer simulation, we can easily obtain curves C_1 and C_2 have a unique positive intersection in the feasible region when $\mathcal{R}_0 > 1$ (see Fig.3 (c)). That is to say, if $\mathcal{R}_0 > 1$, then model (3.2) exists a unique coexistence equilibrium. Curves C_1 and C_2 have no positive intersection in the feasible region when $\mathcal{R}_0 \leq 1$ (see Fig.3 (a) and (b)), i.e., there exists no positive equilibrium when $\mathcal{R}_0 \leq 1$.

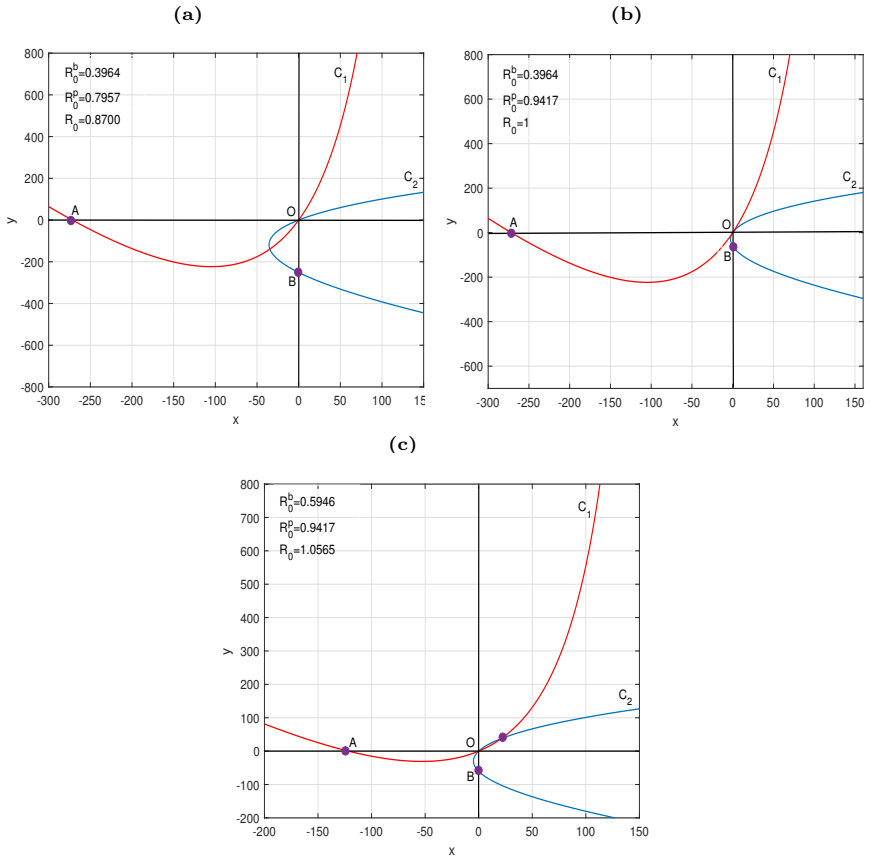

Figure 3. The intersections of curves C_1 and C_2 when $\mathcal{R}_0^b < 1$ and $\mathcal{R}_0^p < 1$.

For case (iii) : $\mathcal{R}_0^b \leq 1$ and $\mathcal{R}_0^p > 1$. In this case, x_1 is not positive and y_1 is positive. Similarity, we get curves C_1 and C_2 exist a unique positive intersection in $\left(0, \frac{\Lambda_b}{\mu_b+d_b}\right) \times \left(0, \frac{\Lambda_p}{\mu_p+d_p}\right)$. Hence, model (3.2) exists a unique coexistence equilibrium, as shown in Fig.4(a).

For case (iv): $\mathcal{R}_0^b > 1$ and $\mathcal{R}_0^p \leq 1$. In this case, x_1 is positive and y_1 is not positive. Moreover, similar to case (iii), curves C_1 and C_2 exists a unique positive intersection in $\left(0, \frac{\Lambda_b}{\mu_b+d_b}\right) \times \left(0, \frac{\Lambda_p}{\mu_p+d_p}\right)$, i.e. model (3.2) exists a unique coexistence equilibrium, as shown in Fig.4(b).

For case (v): $\mathcal{R}_0^b = 1$ and $\mathcal{R}_0^p \leq 1$. In this case, x_1 is equal to zero and y_1 is negative. And the trend of curve C_1 and curve C_2 cannot be determined, so the

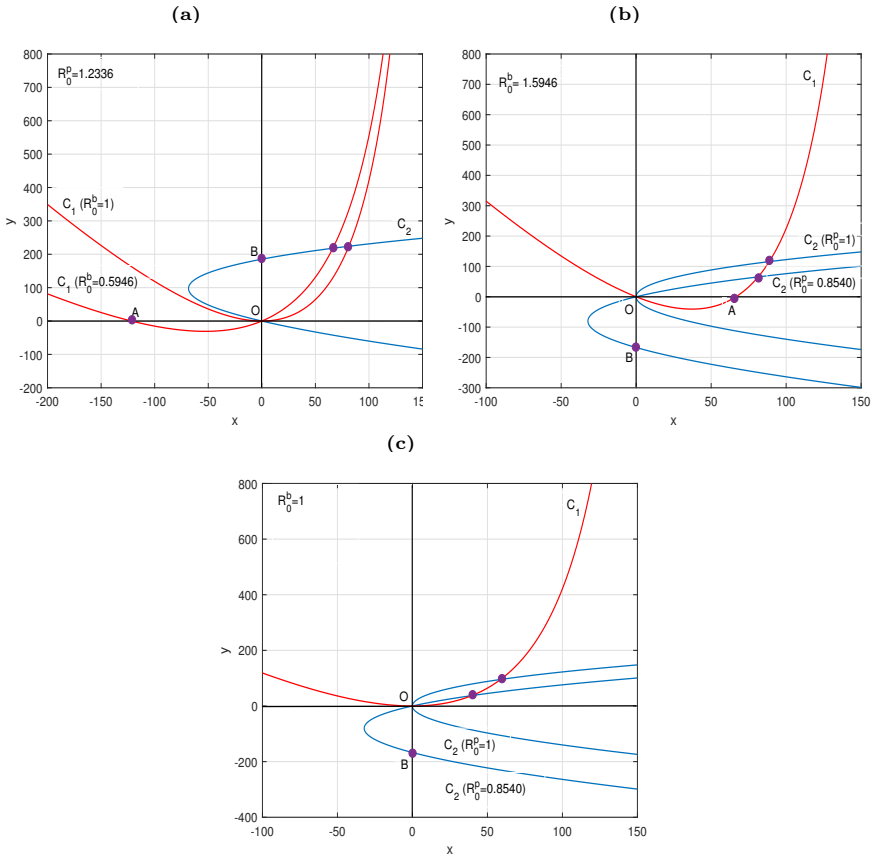

Figure 4. The intersections of curves C_1 and C_2 for cases (iii)-(vi).

existence of the intersection point of the two curves in Ω_{bp} cannot be determined. Therefore, in the following, we will analyze the existence of the intersection point through detailed calculation and combining the basic characteristics of the two curves.

Since $\mathcal{R}_0^b = 1$, by calculation, the equations of curves C_1 and C_2 become the following equations

$$y = \frac{\beta_{bb}^2 x^2}{\beta_{pb}\mu_b - \beta_{pb}\beta_{bb}x}, \qquad x = \frac{\beta_{pp}^2 y^2 + \beta_{pp}\mu_p(1-\mathcal{R}_0^p)y}{\beta_{bp}\mu_p\mathcal{R}_0^p - \beta_{bp}\beta_{pp}y}.$$

Solving the above two equations, we can obtain a cubic equation with x as follows,

$$a_3x^3 + a_2x^2 + a_1x + a_0 = 0, \tag{3.6}$$

where

$$\begin{aligned}
a_3 &= \beta_{pp}^2\beta_{bb}^4\left(1 - \frac{\beta_{bp}\beta_{pb}}{\beta_{bb}\beta_{pp}}\right), \qquad a_0 = -\beta_{bp}\beta_{pb}^2\mu_p\mu_b^2\mathcal{R}_0^p,\\
a_2 &= \beta_{bp}\beta_{pb}\beta_{pp}\beta_{bb}^2\mu_b - \beta_{bp}\beta_{pb}^2\beta_{bb}^2\mu_p\mathcal{R}_0^p - \beta_{pp}\beta_{pb}\beta_{bb}^3\mu_p(1-\mathcal{R}_0^p),\\
a_1 &= 2\beta_{bb}\beta_{bp}\beta_{pb}^2\mu_b\mu_p\mathcal{R}_0^p + \beta_{pp}\beta_{pb}\beta_{bb}^2\mu_b\mu_p(1-\mathcal{R}_0^p).
\end{aligned}$$

It is easy to see that $a_3 > 0$, $a_0 < 0$ and then equation (3.6) has a unique positive root $x^* \in (0, \frac{\Lambda_b}{\mu_b+d_b})$, i.e., curves C_1 and C_2 only has one positive intersection. In addition, due to $x^* \in (0, \frac{\Lambda_b}{\mu_b+d_b})$ and $\mathcal{R}_0^b = 1$, we have $y^* = \beta_{bb}^2 x^{*2}/(\beta_{pb}\mu_b - \beta_{pb}\beta_{bb}x^*) > 0$. It can be concluded from the above analysis that system (3.2) exists a unique coexistence endemic equilibrium, as shown in Fig.4(c).

For case (vi): $\mathcal{R}_0^b \le 1$ and $\mathcal{R}_0^p = 1$. Using a similar discussion as in case (v), we can easily obtain that system (3.2) exists a unique coexistence equilibrium when $\mathcal{R}_0^b \le 1$ and $\mathcal{R}_0^p = 1$.

To sum up the above discussion, we can get the following conclusion.

Theorem 3.2. *If $\mathcal{R}_0 > 1$, then the bird-poultry model* (3.2) *exists a unique coexistence equilibrium $E_+^{bp} = (S_b^*, I_b^*, S_p^*, I_p^*)$.*

Theorem 3.3. *If $\mathcal{R}_0 < 1$, then E_0^{bp} is locally asymptotically stable in Ω_{bp}.*

Proof. The eigenvalue of the Jacobian matrix of model (3.2) at E_0^{bp} are $-\mu_b$, $-\mu_p$, and the roots of the following polynomial

$$\lambda^2 + A_1\lambda + B_1 = 0, \tag{3.7}$$

where

$$\begin{aligned}
A_1 =&\mu_b + d_b - \frac{\Lambda_b\beta_{bb}}{\mu_b} + \mu_p + d_p - \frac{\Lambda_p\beta_{pp}}{\mu_p} = (1-\mathcal{R}_0^b)(\mu_b+d_b) + (1-\mathcal{R}_0^p)(\mu_p+d_p),\\
B_1 =&\left(\mu_b + d_b - \frac{\Lambda_b\beta_{bb}}{\mu_b}\right)\left(\mu_p + d_p - \frac{\Lambda_p\beta_{pp}}{\mu_p}\right) - \frac{\Lambda_b\Lambda_p\beta_{bp}\beta_{pb}}{\mu_b\mu_p}\\
=&(1-\mathcal{R}_0^b)(1-\mathcal{R}_0^p)\left[1 - \frac{\beta_{bp}\beta_{pb}\mathcal{R}_0^b\mathcal{R}_0^p}{\beta_{bb}\beta_{pp}(1-\mathcal{R}_0^b)(1-\mathcal{R}_0^p)}\right](\mu_b+d_b)(\mu_p+d_p).
\end{aligned}$$

It follows from Remark 3.1 that $\mathcal{R}_0 > \max\{\mathcal{R}_0^b, \mathcal{R}_0^p\}$. Hence, if $\mathcal{R}_0 < 1$, we have $\mathcal{R}_0^b < 1$ and $\mathcal{R}_0^p < 1$. Further, A_1 is positive. And, based on $\mathcal{R}_0^b < 1$, $\mathcal{R}_0^p < 1$, we have

$$\mathcal{R}_0 < 1 \Leftrightarrow \frac{\beta_{bp}\beta_{pb}\mathcal{R}_0^b\mathcal{R}_0^p}{\beta_{bb}\beta_{pp}(1-\mathcal{R}_0^b)(1-\mathcal{R}_0^p)} < 1.$$

This implies that B_1 is positive when $\mathcal{R}_0 < 1$. Therefore, both roots of equation (3.7) have a negative real part when $\mathcal{R}_0 < 1$. □

Theorem 3.4. *If $\frac{\beta_{pp}(1-\mathcal{R}_0^p)(\mu_b+d_b)}{\mathcal{R}_0^b\beta_{bp}(\mu_p+d_p)} > 1$ and $\frac{\beta_{bb}(1-\mathcal{R}_0^b)(\mu_p+d_p)}{\mathcal{R}_0^p\beta_{pb}(\mu_b+d_b)} > 1$, then E_0^{bp} is globally asymptotically stable in Ω_{bp}.*

Proof. Choosing the following Lyapunov function

$$L(t) = \left(S_b(t) - S_{b*} - S_{b*}\ln\frac{S_b(t)}{S_{b*}}\right) + I_b(t) + \left(S_p(t) - S_{p*} - S_{p*}\ln\frac{S_p(t)}{S_{p*}}\right) + I_p(t),$$

we have

$$\begin{aligned}\frac{\mathrm{d}L(t)}{\mathrm{d}t} =&\left(1-\frac{S_{b*}}{S_b}\right)\left(\Lambda_b-\beta_{bb}S_bI_b-\beta_{pb}S_bI_p-\frac{\Lambda_b}{S_{b*}S_b}\right)\\&+\left(1-\frac{S_{p*}}{S_p}\right)\left(\Lambda_p-\beta_{pp}S_pI_p-\beta_{bp}S_pI_b-\frac{\Lambda_p}{S_{p*}S_p}\right)\\=&-\frac{\Lambda_b(S_b-S_{b*})^2}{S_bS_{b*}}+[\beta_{bb}S_{b*}I_b+\beta_{pb}S_{b*}I_p-(\mu_b+d_b)I_b]\\=&-\frac{\Lambda_p(S_p-S_{p*})^2}{S_pS_{p*}}+[\beta_{pp}S_{p*}I_p+\beta_{bp}S_{p*}I_b-(\mu_b+d_b)I_p]\\\le&\left[\frac{\Lambda_b\beta_{bb}}{\mu_b}+\frac{\Lambda_p\beta_{bp}}{\mu_p}-(\mu_b+d_b)\right]I_b(t)+\left[\frac{\Lambda_b\beta_{bp}}{\mu_b}+\frac{\Lambda_p\beta_{pp}}{\mu_p}-(\mu_p+d_p)\right]I_p(t)\\=&\left[(\mathcal{R}_0^b-1)(\mu_b+d_b)+\frac{\beta_{bp}\mathcal{R}_0^p}{\beta_{pp}}(\mu_p+d_p)\right]I_b(t)+\left[(\mathcal{R}_0^p-1)(\mu_p+d_p)\right.\\&\left.+\frac{\beta_{pb}\mathcal{R}_0^b}{\beta_{bb}}(\mu_b+d_b)\right]I_p(t).\end{aligned}$$

It is evident that $\mathrm{d}L(t)/\mathrm{d}t<0$ if

$$(\mathcal{R}_0^b-1)(\mu_b+d_b)+\frac{\beta_{bp}\mathcal{R}_0^p}{\beta_{pp}}(\mu_p+d_p)<0\quad\text{and}\quad(\mathcal{R}_0^p-1)(\mu_p+d_p)+\frac{\beta_{pb}\mathcal{R}_0^b}{\beta_{bb}}(\mu_b+d_b)<0,$$

which is equivalent that

$$\frac{\beta_{pp}(1-\mathcal{R}_0^p)(\mu_b+d_b)}{\mathcal{R}_0^b\beta_{bp}(\mu_p+d_p)}>1,\qquad\frac{\beta_{bb}(1-\mathcal{R}_0^b)(\mu_p+d_p)}{\mathcal{R}_0^p\beta_{pb}(\mu_b+d_b)}>1.\tag{3.8}$$

Therefore, if the two inequalities in (3.8) hold, then $dL(t)/dt\le 0$, and it can be verified that $dL(t)/dt=0$, if and only if $S_b=S_{b*}$, $I_b=0$, $S_p=S_{p*}$ and $I_p=0$. That is to say that the largest invariant set in $\{(S_b,I_b,S_p,I_p):dL(t)/dt=0\}$ is the singleton $\{E_0^{bp}\}$. By the LaSalle's invariance principle [29], E_0^{bp} is globally asymptotically stable. □

Remark 3.2. Multiplying the two inequalities in (3.8), we get $\frac{\beta_{bb}\beta_{pp}(1-\mathcal{R}_0^b)(1-\mathcal{R}_0^p)}{\beta_{bp}\beta_{pb}\mathcal{R}_0^b\mathcal{R}_0^p}>1$. It is not hard to see that from $\mathcal{R}_0<1$, we can obtain that this inequality holds. However, we can not obtain that E_0^{bp} is globally asymptotically stable when $R_0<1$, which is still an open problem.

Theorem 3.5. *If $\mathcal{R}_0>1$, then $E_+^{bp}=(S_b^*,I_b^*,S_p^*,I_p^*)$ is globally attractive in Ω_{bp}.*

Proof. Define $\phi(x)=x-\ln x-1$, we have $\phi(x)\ge 0$ for all $x>0$. Let

$$\begin{aligned}W(t)=&\beta_{bp}S_b^*S_p^*I_b^*\phi\left(\frac{S_b}{S_b^*}\right)+\beta_{bp}S_p^*I_b^{*2}\phi\left(\frac{I_b}{I_b^*}\right)\\&+\beta_{pb}S_b^*S_p^*I_p^*\phi\left(\frac{S_p}{S_p^*}\right)+\beta_{pb}S_b^*I_p^{*2}\phi\left(\frac{I_p}{I_p^*}\right).\end{aligned}$$

Then

$$\begin{aligned}\frac{\mathrm{d}W(t)}{\mathrm{d}t} =& -\beta_{bp}S_p^*I_b^*\mu_b\frac{(S_b-S_b^*)^2}{S_b}+\beta_{bp}S_p^*I_b^*(1-\frac{S_b^*}{S_b})\Big[\beta_{bb}S_b^*I_b^*+\beta_{pb}S_b^*I_p^*\\ &-\beta_{bb}S_bI_b-\beta_{pb}S_bI_p\Big]+\beta_{bp}S_p^*I_b^*\left(1-\frac{I_b^*}{I_b}\right)\Big[\beta_{bb}S_bI_b+\beta_{pb}S_bI_p\\ &-(\mu_b+d_b)I_b\Big]-\beta_{pb}S_b^*I_p^*\mu_p\frac{(S_p-S_p^*)^2}{S_p}+\beta_{pb}S_b^*I_p^*\left(1-\frac{S_p^*}{S_p}\right)\\ &\times\left[\beta_{pp}S_p^*I_p^*+\beta_{bp}S_p^*I_b^*-\beta_{pp}S_pI_p-\beta_{bp}S_pI_b\right]+\beta_{pb}S_b^*I_p^*\left(1-\frac{I_p^*}{I_p}\right)\\ &\times\left[\beta_{pp}S_pI_p+\beta_{bp}S_pI_b-(\mu_p+d_p)I_p\right]\\ \le&\beta_{bp}\beta_{bb}S_b^*S_p^*I_b^{*2}\left[2-\frac{S_b^*}{S_b}-\frac{S_b}{S_b^*}\right]+\beta_{pp}\beta_{pb}S_b^*S_p^*I_p^{*2}\left[2-\frac{S_p^*}{S_p}-\frac{S_p}{S_p^*}\right]\\ &+\beta_{bp}\beta_{pb}S_b^*S_p^*I_b^*I_p^*\left[2+\frac{I_p}{I_p^*}-\frac{S_b^*}{S_b}-\frac{I_b}{I_b^*}-\frac{S_bI_pI_b^*}{S_b^*I_p^*I_b}\right]\\ &+\beta_{bp}\beta_{pb}S_b^*S_p^*I_b^*I_p^*\left[2+\frac{I_b}{I_b^*}-\frac{S_p^*}{S_p}-\frac{I_p}{I_p^*}-\frac{S_pI_bI_p^*}{S_p^*I_b^*I_p}\right]\\ \le&-\beta_{bp}\beta_{pb}S_b^*S_p^*I_b^*I_p^*\left(\phi\left(\frac{S_b^*}{S_b}\right)+\phi\left(\frac{S_p^*}{S_p}\right)+\phi\left(\frac{S_bI_pI_b^*}{S_b^*I_p^*I_b}\right)+\phi\left(\frac{S_pI_bI_p^*}{S_p^*I_b^*I_p}\right)\right).\end{aligned}$$

Therefore, if $R_0>1$, then $dW(t)/dt\le 0$, and it can be verified that $dW(t)/dt=0$, if and only if $S_b=S_b^*$, $I_b=I_b^*$, $S_p=S_p^*$ and $I_p=I_p^*$. That is to say that the largest invariant set in $\{(S_b,I_b,S_p,I_p):dW(t)/dt=0\}$ is the singleton $\{E_+^{bp}\}$. By the LaSalle's invariance principle [29], E_+^{bp} is globally attractive for model (3.2). □

4. Analysis of the whole model

In this section, we discuss the threshold dynamics for the whole model (2.1). Clearly, model (2.1) always has a disease-free equilibrium $E_0=(\frac{\Lambda_b}{\mu_b},0,\frac{\Lambda_p}{\mu_p},0,\frac{\Lambda_h}{\mu_h},0,0)$, and has a unique positive equilibrium $E_+^*=(S_b^*,I_b^*,S_p^*,I_p^*,S_h^*,I_h^*,R_h^*)$ when $\mathcal{R}_0>1$, where

$$S_h^*=\frac{\Lambda_h}{\beta_{bh}I_b^*+\beta_{ph}I_p^*+\mu_h},\qquad I_h^*=\frac{\Lambda_h-\mu_hS_h^*}{\gamma_h+\mu_h+d_h},\qquad R_h^*=\frac{\gamma_h(\Lambda_h-\mu_hS_h^*)}{\mu_h(\gamma_h+\mu_h+d_h)}.$$

The positivity of S_h^* follows from Theorem 3.3. Let $E^*=(\widetilde{S}_b^*,\widetilde{I}_b^*,\widetilde{S}_p^*,\widetilde{I}_p^*,\widetilde{S}_h^*,\widetilde{I}_h^*,\widetilde{R}_h^*)$ be an arbitrary equilibrium of model (2.1). Then the Jacobian matrix at E^* of the corresponding model (2.1) is

$$J(E^*)=\begin{pmatrix}J_{11}&0\\J_{12}&J_{22}\end{pmatrix},$$

where J_{11} and J_{22} are given by

$$J_{11} = \begin{pmatrix} -\beta_{bb}\widetilde{I}_b^* - \beta_{pb}\widetilde{I}_p^* - \mu_b & -\beta_{bb}\widetilde{S}_b^* & 0 & -\beta_{pb}\widetilde{S}_b^* \\ \beta_{bb}\widetilde{I}_b^* + \beta_{pb}\widetilde{I}_p^* & \beta_{bb}\widetilde{S}_b^* - (\mu_b + d_b) & 0 & \beta_{pb}\widetilde{S}_b^* \\ 0 & -\beta_{bp}\widetilde{S}_p^* & -\beta_{pp}\widetilde{I}_p^* - \beta_{bp}\widetilde{I}_b^* - \mu_p & -\beta_{pp}\widetilde{S}_p^* \\ 0 & \beta_{bp}\widetilde{S}_p^* & \beta_{pp}\widetilde{I}_p^* + \beta_{bp}\widetilde{I}_b^* & \beta_{pp}\widetilde{S}_p^* - (\mu_p + d_p) \end{pmatrix}$$

and

$$J_{22} = \begin{pmatrix} -\beta_{bh}\widetilde{I}_b^* - \beta_{ph}\widetilde{I}_p^* - \mu_h & 0 & 0 \\ \beta_{bh}\widetilde{I}_b^* + \beta_{ph}\widetilde{I}_p^* & -(\gamma_h + d_h + \mu_h) & 0 \\ 0 & \gamma_h & -\mu_h \end{pmatrix}.$$

Obviously, the eigenvalues of the matrix J_{22} have negative real parts, hence, the stability of the equilibria is determined by the eigenvalues of the matrix J_{11}, which is also the Jacobian matrix of the first four equations of model (2.1) at an arbitrary equilibrium $E_{bp}^* = (\widetilde{S}_b^*, \widetilde{I}_b^*, \widetilde{S}_p^*, \widetilde{I}_p^*)$. Therefore, we can obtain the following results.

Theorem 4.1. *The following statements are valid:*

(i) If $\mathcal{R}_0 < 1$, then E_0 is locally asymptotically stable in Ω;

(ii) If $\frac{\beta_{pp}(1-\mathcal{R}_0^p)(\mu_b+d_b)}{\mathcal{R}_0^b\beta_{bp}(\mu_p+d_p)} > 1$ and $\frac{\beta_{bb}(1-\mathcal{R}_0^b)(\mu_p+d_p)}{\mathcal{R}_0^p\beta_{pb}(\mu_b+d_b)} > 1$, then E_0 is globally asymptotically stable in Ω.

(iii) If $\mathcal{R}_0 > 1$, then $E_+^* = (S_b^*, I_b^*, S_p^*, I_p^*, S_h^*, I_h^*, R_h^*)$ is globally attractive in Ω.

Proof. (i). From Theorem 3.3 and the fact that all eigenvalues of the matrix J_{22} have negative reals parts, the proof is immediate.

(ii). From Theorem 3.4, we see that if $\frac{\beta_{pp}(1-\mathcal{R}_0^p)(\mu_b+d_b)}{\mathcal{R}_0^b\beta_{bp}(\mu_p+d_p)} > 1$ and $\frac{\beta_{bb}(1-\mathcal{R}_0^b)(\mu_p+d_p)}{\mathcal{R}_0^p\beta_{pb}(\mu_b+d_b)} > 1$, then

$$\lim_{t\to\infty}(S_b(t), I_b(t), S_p(t), I_p(t)) = (S_{b*}, 0, S_{p*}, 0).$$

Consider the following limit system

$$\begin{cases} \dfrac{\mathrm{d}S_h(t)}{\mathrm{d}t} = \Lambda_h - \mu_h S_h(t), \\ \dfrac{\mathrm{d}I_h(t)}{\mathrm{d}t} = -(\gamma_h + \mu_h + d_h)I_h(t), \\ \dfrac{\mathrm{d}R_h(t)}{\mathrm{d}t} = \gamma_h I_h(t) - \mu_h R_h(t). \end{cases} \tag{4.1}$$

Solving the first two equations of model (4.1), we get

$$S_h(t) = S_{h0}e^{-\mu_h t} + \frac{\Lambda_h}{\mu_h}, \qquad I_h(t) = I_{h0}e^{-(\gamma_h+\mu_h+d_h)t}.$$

It follows that $S_h(t) \to S_h^*$ and $I_h(t) \to 0$ as $t \to \infty$. We further consider the limit equation of $R_h(t)$, $\mathrm{d}R_h(t)/\mathrm{d}t = -\mu_h R_h(t)$. Thus, we have $R_h(t) \to 0$ as $t \to \infty$.

(iii). From Theorem 3.5, we see that if $\mathcal{R}_0 > 1$, then

$$\lim_{t\to\infty}(S_b(t), I_b(t), S_p(t), I_p(t)) = (S_b^*, I_b^*, S_p^*, I_p^*).$$

Consider the following limit equation,

$$\frac{\mathrm{d}S_h(t)}{\mathrm{d}t} = \Lambda_h - (\beta_{bh} I_b^* + \beta_{ph} I_p^* + \mu_h) S_h(t). \tag{4.2}$$

Solving equation (4.2), we get

$$S_h(t) = S_{h0} e^{-(\beta_{bh} I_b^* + \beta_{ph} I_p^* + \mu_h)t} + \frac{\Lambda}{\beta_{bh} I_b^* + \beta_{ph} I_p^* + \mu_h}.$$

It follows that $S_h(t) \to S_h^*$ as $t \to \infty$. Using a similar argument, we can show that $\lim_{t\to\infty} I_h(t) = I_h^*$ and $\lim_{t\to\infty} R_h(t) = R_h^*$. □

5. Sensitivity analysis and optimal control problem

Based on the discussion in Sections 3 and 4, we can conclude that the basic reproduction number $\mathcal{R}_0$ is an important threshold value for determining whether the disease becomes endemic or extinct. However, there are many parameters in the expression of basic reproduction number $\mathcal{R}_0$, but which parameters have the greatest impact on the basic regeneration number $\mathcal{R}_0$? In other words, biologically speaking, what measures are more likely to be taken to control the spread of diseases? In order to settle this problem, in this section, we firstly discuss the sensitivity of some parameters in model (2.1) to the basic reproduction number $\mathcal{R}_0$, and then propose a corresponding control problem based on the results of sensitivity analysis. In order to conduct sensitivity analysis, we first need to introduce the definition of sensitivity index.

Definition 5.1. The normalized forward sensitivity index of a variable, u, which depends differentiable on a parameter, p, is defined as,

$$\gamma_p^u := \frac{\partial u}{\partial p} \times \frac{p}{u}. \tag{5.1}$$

Table 1. Sensitivity index of the reproduction number $\mathcal{R}_0$.

Param.	Description	Value
Λ_p	Recruitment rate of poultry population	0.6515
β_{bb}	Transmission rate from bird to bird	0.2463
β_{pb}	Transmission rate from poultry to bird	0.1022
β_{pp}	Transmission rate from poultry to poultry	0.5493
β_{bp}	Transmission rate from bird to poultry	0.1022
μ_p	Death rate of poultry (including natural death and culling)	-0.8526

Due to the practical biological significance of certain parameters, we mainly focus on the sensitivity of parameters shown in Table 1. Based on the study in [5, 19, 32], we fix some parameter values $\Lambda_b = 10^8/520$, $\beta_{bb} = 2.0 \times 10^{-9}$, $\beta_{pb} = 9.3114 \times 10^{-10}$, $\mu_b = 1/520$, $d_b = 0.18$, $\Lambda_p = 1.0438 \times 10^8/6$, $\beta_{pp} = 3.8164 \times 10^{-9}$, $\beta_{bp} = 6.3243 \times 10^{-10}$, $\mu_p = 1/8$ and $d_p = 0.28$. Then using the equation (5.1), we

can obtain the sensitivity index of the basic reproduction number $\mathcal{R}_0$ regarding some key parameters of model (2.1) as shown in Table 1 and Figure 5. From e Figure 5, we can see that $\mathcal{R}_0$ is the most sensitive to poultry mortality μ_p, followed by the recruitment rate of poultry Λ_p, and finally, the rate of transmission poultry-to-poultry β_{pp} and bird-to-bird β_{bb}. Specifically, Table 1 shows that a reduction of the poultry death rate by 10% increases $\mathcal{R}_0$ by 8.526%; the increase in the recruitment rate of poultry by 10% would increase $\mathcal{R}_0$ by 6.515%; a reduction of the rate of transmission poultry-to-poultry and bird-to-bird by 10% decreases $\mathcal{R}_0$ by 5.493% and 2.463%, respectively.

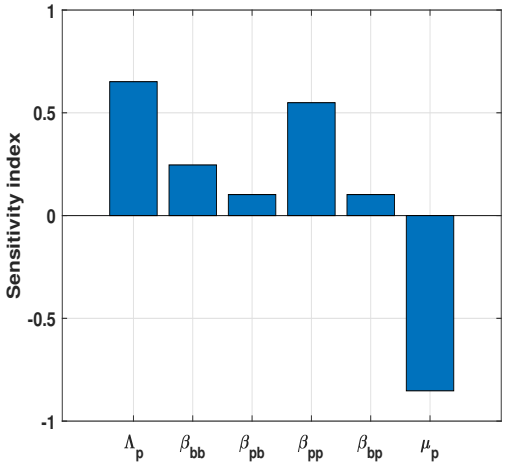

Figure 5. Sensitivity indices of $\mathcal{R}_0$ to parameters for model (2.1).

Although birds are one of the major potential vectors for the spread of highly pathogenic avian influenza, given their importance to the ecosystem, the removal and killing of birds can easily cause an imbalance in the ecosystem and make it difficult to maintain. Therefore, combined with the above sensitivity analysis results, the effective strategy to control the transmission of avian influenza virus is to adopt relevant control on poultry. The most effective strategy is to increase the mortality rate of poultry by large-scale killing, followed by reducing the recruitment rate of susceptible poultry through immunization. The third is to reduce the contact rate between birds and poultry (such as changing the free-range poultry to captivity, and disinfecting the living environment of captive poultry).

In terms of the results of the sensitivity analysis, we design a control model to the optimal level of effort required for controlling the transmission of avian influenza virus. We introduce four time-dependent control strategies, $u_1(t)$, $u_2(t)$, $u_3(t)$ and $u_4(t)$ regarding the recruitment rate of susceptible poultry, the cull rate of susceptible poultry, the cull rate of infected poultry and the personal protection rate of susceptible human. $u_1(t) \in [0, 1]$ measures the level of reduction in the number of susceptible poultry, which can be achieved by increasing the immunization ratio of susceptible poultry. $u_1(t) = 1$ indicates that full immunization coverage of poultry population(including those in concentrated farms and those in free-range farming households). The costs associated with this control strategy include raising the

public awareness of the disease through publicity and education, so that farmers can regularly vaccinate hatching poultry. $u_2(t) \in [0,1]$ and $u_3(t) \in [0,1]$ represent the level of culling susceptible poultry and infected poultry, respectively, which are common control measures during avian influenza epidemics. Here $u_2(t) = u_3(t) = 1$ means culling all poultry, which will bring huge economic losses. $u_4(t)$ measures the level of successful prevention (personal protection) through public health education. Personal protection includes wearing protective equipment such as masks and gloves when in contact with birds or poultry, and even avoiding contact with live birds or poultry to minimize or eliminate poultry-human and bird-human direct contacts. Therefore, we analysis the following avian influenza model with control strategy terms:

$$\begin{cases} \dfrac{\mathrm{d}S_b(t)}{\mathrm{d}t} =\Lambda_b - \beta_{bb}S_b(t)I_b(t) - \beta_{pb}S_b(t)I_p(t) - \mu_b S_b(t), \\ \dfrac{\mathrm{d}I_b(t)}{\mathrm{d}t} =\beta_{bb}S_b(t)I_b(t) + \beta_{pb}S_b(t)I_p(t) - (\mu_b + d_b)I_b(t), \\ \dfrac{\mathrm{d}S_p(t)}{\mathrm{d}t} =(1-u_1(t))\Lambda_p - \beta_{pp}S_p(t)I_p(t) - \beta_{bp}S_p(t)I_b(t) - (\mu_p + u_2(t))S_p(t), \\ \dfrac{\mathrm{d}I_p(t)}{\mathrm{d}t} =\beta_{pp}S_p(t)I_p(t) + \beta_{bp}S_p(t)I_b(t) - (\mu_p + d_p + u_3(t))I_p(t), \\ \dfrac{\mathrm{d}S_h(t)}{\mathrm{d}t} =\Lambda_h - (1-u_4(t))S_h(t)(\beta_{bh}I_b(t) + \beta_{ph}I_p(t)) - \mu_h S_h(t), \\ \dfrac{\mathrm{d}I_h(t)}{\mathrm{d}t} =(1-u_4(t))S_h(t)(\beta_{bh}I_b(t) + \beta_{ph}I_p(t)) - (\gamma_h + d_h + \mu_h)I_h(t), \\ \dfrac{\mathrm{d}R_h(t)}{\mathrm{d}t} =\gamma_h I_h(t) - \mu_h R_h(t). \end{cases} \tag{5.2}$$

Obviously, when $u_i(t)(i = 1,2,3,4)$ are constants, the dynamic behavior of model (5.2) is similar to the dynamic behavior of model (2.1), so we do not discuss it. We focus on minimizing susceptible poultry and infected poultry, as well as minimizing infected human. Therefore, an optimal control problem with the objective is given by

$$\begin{aligned} \min J(u_1,u_2,u_3,u_4) = \int_0^{t_{end}} & [q_1 S_p(t) + q_2 I_p(t) + q_3 I_h(t) + q_4 u_1^2 \\ & + q_5 u_2^2 + q_6 u_3^2 + q_7 u_4^2]\mathrm{d}t, \end{aligned} \tag{5.3}$$

where q_1, q_2 and q_3 represent weight constants of the number of susceptible poultry, infected poultry and infected human; q_4, q_5 and q_6 are weight constants for poultry immunization, culling of susceptible poultry and culling of infected poultry , respectively; q_7 is a weight constant for the personal protection of susceptible human. We will investigate optimal control functions $(u_1^*, u_2^*, u_3^*, u_4^*)$ such that

$$J(u_1^*, u_2^*, u_3^*, u_4^*) = \min\big(J(u_1,u_2,u_3,u_4) | (u_1,u_2,u_3,u_4) \in \Gamma\big), \tag{5.4}$$

where $\Gamma = \{(u_1,u_2,u_3,u_4) | u_i(t)$ is Lebesgue measurable on $[0,t_{end}]$ and $0 \le u_i(t) \le 1, i = 1,2,3,4\}$ is the control strategy set. Using the similar arguments as in [27], we have the following result for the existence of an optimal control about (5.2) and (5.3).

Theorem 5.1. *There exists an optimal control set $(u_1^*, u_2^*, u_3^*, u_4^*) \in \Gamma$ with corresponding nonnegative states $(S_b, I_b, S_p, I_p, S_h, I_h, R_h)$ that minimize the objective*

functional $J(u_1(t), u_2(t), u_3(t), u_4(t))$.

Proof. The positivity and uniform boundedness of the state variables as well as the controls on $[0, t_{end}]$ entail the existence of a minimizing sequence:

$$J\left(u_1^n(t), u_2^n(t), u_3^n(t), u_4^n(t)\right),$$

such that

$$\begin{aligned}&\lim_{n\longrightarrow\infty} J\left(u_1^n(t), u_2^n(t), u_3^n(t), u_4^n(t)\right)\\ &\quad= \inf_{\left(u_1^n(t), u_2^n(t), u_3^n(t), u_4^n(t)\right)\in\Gamma} J\left(u_1^n(t), u_2^n(t), u_3^n(t), u_4^n(t)\right).\end{aligned}$$

The boundedness of all the state and control variables implies that all the derivatives of the state variables are also bounded. If the corresponding sequence of state variables is denoted by $(S_b, I_b, S_p, I_p, S_h, I_h, R_h)$, then all state variables are Lipschitz continuous with the same Lipschitz constant. This implies that the sequence $(S_b, I_b, S_p, I_p, S_h, I_h, R_h)$ is uniformly equicontinuous in $[0, t_{end}]$. Following the approach in [30], the state sequence has a subsequence that converges uniformly to $(S_b, I_b, S_p, I_p, S_h, I_h, R_h)$ in $[0, t_{end}]$. In addition, we can establish that the control sequence $u^n = \left(S_b^n, I_b^n, S_p^n, I_p^n, S_h^n, I_h^n, R_h^n\right)$ has a subsequence that converges weakly in $L^2(0, t_{end})$. Let $(u_1^*, u_2^*, u_3^*, u_4^*) \in \Gamma$ be such that $u_i^n \longrightarrow u_i^*$ weakly in $L^2(0, t_{end})$ for $i = 1, 2, 3, 4$. Applying the lower semicontinuity of norms in weak L^2, we have

$$\|u_i^*\|_{L^2}^2 \leq \liminf_{n\to\infty} \|u_i^n(t)\|_{L^2}^2.$$

This means that

$$\begin{aligned}J(u_1^*, u_2^*, u_3^*, u_4^*) \leq \lim_{n\to\infty} \int_0^{t_{end}} &[q_1 S_p^n(t) + q_2 I_p^n(t) + q_3 I_h^n(t)\\ &+ q_4 u_1^n + q_5 u_2^n + q_6 u_3^n + q_7 u_4^n]\mathrm{d}t,\end{aligned}$$

which completes the proof. □

In the following part, we derive necessary conditions for an optimal control and formulate an optimality system that characterizes the optimal control using upper and lower bound techniques. According to the Ponteyagins maximum principle [31], the necessary conditions for an optimal control problem can be obtained. The principle converts system (5.2) and equation (5.3) into a problem of maximizing pointwise Hamilton H, with respect to u_1, u_2, u_3, and u_4 defined by :

$$H = q_1 S_p(t) + q_2 I_p(t) + q_3 I_h(t) + q_4 u_1^2 + q_5 u_2^2 + q_6 u_3^2 + q_7 u_4^2 + \sum_{i=1}^{7} \lambda_i f_i, \qquad (5.5)$$

where f_i is the right-hand side for the different equation of i-th state variable. By Ponteyagins maximum principle and the existence result for the optimal control, we derive the following result of the necessary conditions for the optimal control problem.

Theorem 5.2. *For the optimal solution* $(\tilde{S}_b(\cdot), \tilde{I}_b(\cdot), \tilde{S}_p(\cdot), \tilde{I}_p(\cdot), \tilde{S}_h(\cdot), \tilde{I}_h(\cdot), \tilde{H}_h(\cdot), \tilde{R}_h(\cdot))$ *associated with an optimal control* $J^*(u_1^*, u_2^*, u_3^*, u_4^*)$ *on* $[0, t_{end}]$, *there exist adjoint functions,* $\lambda_i(t)$, *for* $i = 1, 2, \cdots, 7$, *satisfying*

$$\begin{cases} \dfrac{\mathrm{d}\lambda_1(\cdot)}{\mathrm{d}t} =(\lambda_1-\lambda_2)(\beta_{bb}\tilde{I}_b+\beta_{pb}\tilde{I}_p)+\lambda_1\mu_b, \\ \dfrac{\mathrm{d}\lambda_2(\cdot)}{\mathrm{d}t} =(\lambda_1-\lambda_2)\beta_{bb}\tilde{S}_b+(\lambda_3-\lambda_4)\beta_{bp}\tilde{S}_p+(\lambda_5-\lambda_6)\beta_{bh}\tilde{S}_h(1-u_4^*) \\ \qquad\quad +\lambda_2(\mu_b+d_b), \\ \dfrac{\mathrm{d}\lambda_3(\cdot)}{\mathrm{d}t} =-q_1+(\lambda_3-\lambda_4)(\beta_{pp}\tilde{I}_p+\beta_{bp}\tilde{I}_b)+(\mu_p+u_2^*)\lambda_3, \\ \dfrac{\mathrm{d}\lambda_4(\cdot)}{\mathrm{d}t} =-q_2+(\lambda_1-\lambda_2)\beta_{pb}\tilde{S}_b+(\lambda_3-\lambda_4)\beta_{pp}\tilde{S}_p+(\lambda_5-\lambda_6)\beta_{ph}\tilde{S}_h \\ \qquad\quad \times(1-u_4^*)+\lambda_4(\mu_p+d_p+u_3^*), \end{cases} \tag{5.6}$$

$$\begin{cases} \dfrac{\mathrm{d}\lambda_5(\cdot)}{\mathrm{d}t} =(\lambda_5-\lambda_6)(\beta_{ph}\tilde{I}_p+\beta_{bh}\tilde{I}_b)(1-u_4^*)+\lambda_5\mu_h, \\ \dfrac{\mathrm{d}\lambda_6(\cdot)}{\mathrm{d}t} =-q_3+(\lambda_6-\lambda_7)\gamma_h+\lambda_6(\mu_h+d_h), \\ \dfrac{\mathrm{d}\lambda_7(\cdot)}{\mathrm{d}t} =\lambda_7\mu_h, \end{cases}$$

and the terminal conditions are $\lambda_i(t_{end})=0$, $i=1,2,\cdots,7$. *Furthermore, optimal control strategies* u_1^*, u_2^*, u_3^* *and* u_4^* *are given by*

$$u_1^*=\min\left\{1,\max\left\{0,\frac{\lambda_3\Lambda_p}{2q_4}\right\}\right\}, u_2^*=\min\left\{1,\max\left\{0,\frac{\lambda_3\tilde{S}_p}{2q_5}\right\}\right\},$$
$$u_3^*=\min\left\{1,\max\left\{0,\frac{\lambda_4\tilde{I}_p}{2q_6}\right\}\right\},$$
$$u_4^*=\min\left\{1,\max\left\{0,\frac{(\lambda_6-\lambda_5)(\beta_{ph}\tilde{I}_p+\beta_{bh}\tilde{I}_b)\tilde{S}_h}{2q_7}\right\}\right\}.$$

Proof. Adjoint equations and transversality conditions can be obtained using Pontryagin's Maximum Principle such that

$$\begin{aligned} \frac{\mathrm{d}\lambda_1(t)}{\mathrm{d}t}&=-\frac{\partial H}{\partial S_b}, & \lambda_1(t_{end})&=0, \\ \frac{\mathrm{d}\lambda_2(t)}{\mathrm{d}t}&=-\frac{\partial H}{\partial I_b}, & \lambda_2(t_{end})&=0, \\ \cdots & & \cdots & \\ \frac{\mathrm{d}\lambda_7(t)}{\mathrm{d}t}&=-\frac{\partial H}{\partial R_h}, & \lambda_7(t_{end})&=0. \end{aligned}$$

The optimal control strategies u_1^*,u_2^*,u_3^*,u_4^* can be solved from the optimality conditions

$$\frac{\partial H}{\partial u_1}=0, \qquad \frac{\partial H}{\partial u_2}=0, \qquad \frac{\partial H}{\partial u_3}=0, \qquad \frac{\partial H}{\partial u_4}=0.$$

□

6. Numerical simulation

6.1. Verification of theoretical results

In this subsection, to illustrate the theoretical results, two examples are carried out using the Runge–Kutta method in the software MATLAB routines with different parameters values. Based on the actual biological significance of the parameters, we need to fix some parameters as in Table 2.

Table 2. Values of some parameters in model (2.1)

Parameter	Value	Reference	Parameter	Value	Reference
Λ_b	$10^8/520$	[32]	μ_b	$1/520$	[32]
d_b	0.18	[5]	d_p	0.28	[19]
Λ_h	$2.269741 \times 10^8/3640$	[32]	μ_h	$1/3640$	[5]
γ_h	0.36	[32]	d_h	$7/3.3$	[32]

Example 1: In order to verify the globally asymptotically stability of the disease-free equilibrium E_0 for system (2.1), we select a set of parameter values from [19]: $\beta_{bb} = 1.3\times10^{-9}, \beta_{pb} = 7.3114\times10^{-10}$, $\Lambda_p = 0.9\times10^8/6$, $\beta_{pp} = 2.3\times10^{-9}$, $\beta_{bp} = 4.3243 \times 10^{-10}$, $\mu_p = 1/8$, $\beta_{bh} = 2.6245 \times 10^{-10}$ and $\beta_{ph} = 1.1542 \times 10^{-9}$. It is easy to calculate that the threshold values $R_0^b = 0.7146 < 1$, $R_0^p = 0.6815 < 1$ and $\frac{\beta_{pp}(1-R_0^p)(\mu_b+d_b)}{R_0^b\beta_{bp}(\mu_p+d_p)} = 1.0649 > 1$, $\frac{\beta_{bb}(1-R_0^b)(\mu_p+d_p)}{R_0^p\beta_{pb}(\mu_b+d_b)} = 1.6578 > 1$, then model (2.1) has a unique globally asymptotically stable disease-free equilibrium by Theorem 4.1, which is verified here by Figs. 6 (a) and (b). However, in this case, we calculate that $R_0 = 0.9256 < 1$, i.e., indicating that the disease-free equilibrium E_0 is globally asymptotically stable by numerical simulations but it is still an open problem in theoretical analysis.

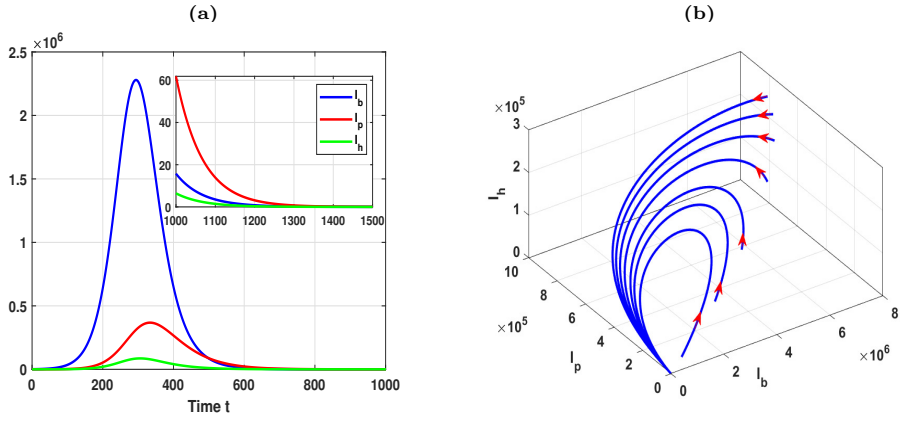

Figure 6. The global asymptotically stability of the disease-free equilibrium E_0

Example 2: In order to verify the globally asymptotically stability of the endemic equilibrium E_0 for system (2.1), we choose $\beta_{bb} = 2.0 \times 10^{-9}$, $\beta_{pb} =$

9.3114×10^{-10}, $\Lambda_p = 1.0438 \times 10^8/6$, $\beta_{pp} = 3.8164 \times 10^{-9}$, $\beta_{bp} = 6.3243 \times 10^{-10}$, $\mu_p = 1/8$, $\beta_{bh} = 2.6245 \times 10^{-10}$ and $\beta_{ph} = 1.1542 \times 10^{-9}$. It is easy to calculate that the threshold values $R_0^b = 1.0994 > 1$, $R_0^p = 1.3115 > 1$ and $R_0 = 1.5554 > 1$, then model (2.1) has a unique globally asymptotically stable endemic equilibrium by Theorem 4.1, which is verified here by Figs. 7 (a) and (b).

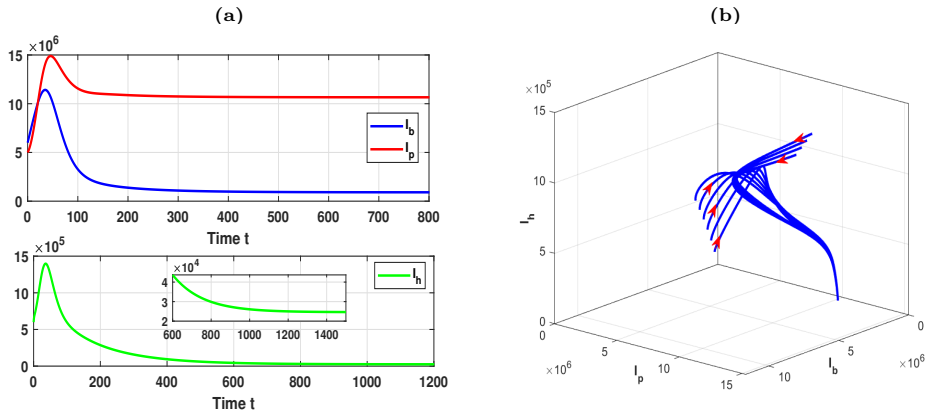

Figure 7. The global asymptotically stability of the endemic equilibrium E_+^*

6.2. Visualization of the impact of various parameters on model dynamics

In this subsection, we mainly visualize the impact of some key parameters on model dynamics based on the discussion in Section 5. Firstly, we keep the same parameters as in Example 2 except the recruitment rate Λ_p to investigate its impact on model dynamics. Taking $\Lambda_p = 1.0438 \times 10^8/7$, $\Lambda_p = 0.9438 \times 10^8/7$, $\Lambda_p = 0.8438 \times 10^8/7$, and $\Lambda_p = 0.7438 \times 10^8/7$, the evolution solutions of I_b, I_p and I_h for system (2.1) are obtained (see Figs.8(a)-(c)), respectively. Obviously, the peak values of infected patients, infected poultry, and infected birds increase as Λ_p increases, and the time they reach the peaks also migrate with the increase of Λ_p. Biologically, during the outbreak of avian influenza, reducing the recruitment rate of susceptible poultry can effectively reduce the number of infected patients, infected birds, and infected poultry. At the same time, it can delay the time of the pandemic and help disease control departments take relevant control measures in time.

In addition, while keeping the other parameters in Example 2 unchanged, we take three cases for the values of Λ_p, β_{bp} and β_{bh}, and then calculate the corresponding values of R_0^b, R_0^p and R_0 to get the final state values for infected humans, infected birds, and infected poultry(see Table 3). At the same time, the evolution solutions of system (2.1) for infected humans, infected birds, and infected poultry are respectively obtained (see Figs.8(d)-(f)). Contrasting Case I and Case II in Table 3, we can easily obtain that $R_0^b > 1$, $R_0^p > 1$, and $R_0 > 1$ change to $R_0^b > 1$, $R_0^p < 1$, and $R_0 > 1$. The final size of infected birds, infected poultry and infected human has decreased, which means that the decrease of the recruitment rate Λ_p can effectively reduce the final scale of the epidemic outbreak but can not control the disease transmission even if $R_0^p < 1$. Moreover, contrasting Case II and Case

Table 3. Three cases to indicate the influence of Λ_p on disease dynamics

Case	Λ_p	β_{bp}	β_{bh}	R_0^b	R_0^p	R_0	$I_b(\infty)$	$I_p(\infty)$	$I_h(\infty)$
I	$1.0438 \times 10^8/7$	6.3243×10^{-10}	2.6245×10^{-10}	1.0994	1.1242	1.4208	806961	4929940	24010.6
II	$0.8438 \times 10^8/7$	6.3243×10^{-10}	2.6245×10^{-10}	1.0994	0.9087	1.2976	464511	621240	18931
III	$0.8438 \times 10^8/7$	0	0	1.0994	0.9087	1.0994	95457.6	0	0

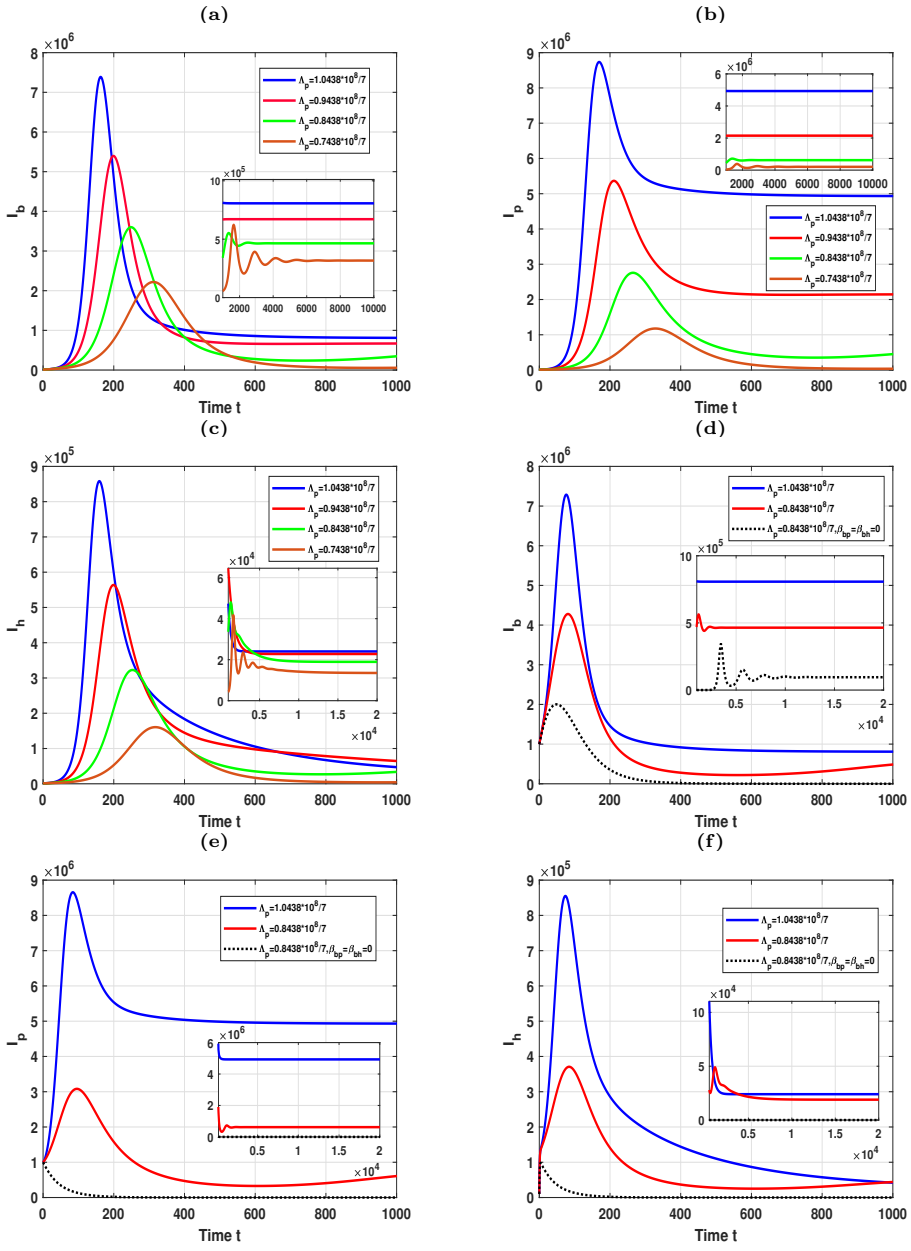

Figure 8. The impact of Λ_p on the solutions related to infected population for model (2.1)

III in Table 3, even though the basic reproduction numbers $R_0^b > 1$, $R_0^p < 1$, and $R_0 > 1$ unchanged, the final scale of the infected scale of infected poultry and infected humans comes to zero. Biologically, keeping the same recruitment rate Λ_p and cutting off the transmission from birds to poultry and humans($\beta_{bp} = \beta_{bh} = 0$) can make the final scale of the infected poultry and infected humans zero even if the basic reproduction numbers $R_0^b > 1$, $R_0^p < 1$, and $R_0 > 1$.

Similarly, we keep the same parameters in Example 2 except the death rate μ_p to investigate its impact on model dynamics. Taking $\mu_p = 1/8$, $\mu_p = 1/7.5$, $\mu_p = 1/7$, $\mu_p = 1/6.5$ and $\mu_p = 1/6$, the evolution solutions of I_b, I_p and I_h for system (2.1) are obtained (see Figs.9(a)), respectively. Obviously, the peak values of infected patients, infected poultry, and infected birds decrease with the increase of μ_p. Biologically, during the outbreak of avian influenza, increasing the death rate of poultry can effectively reduce the number of infected patients, infected birds, and infected poultry.

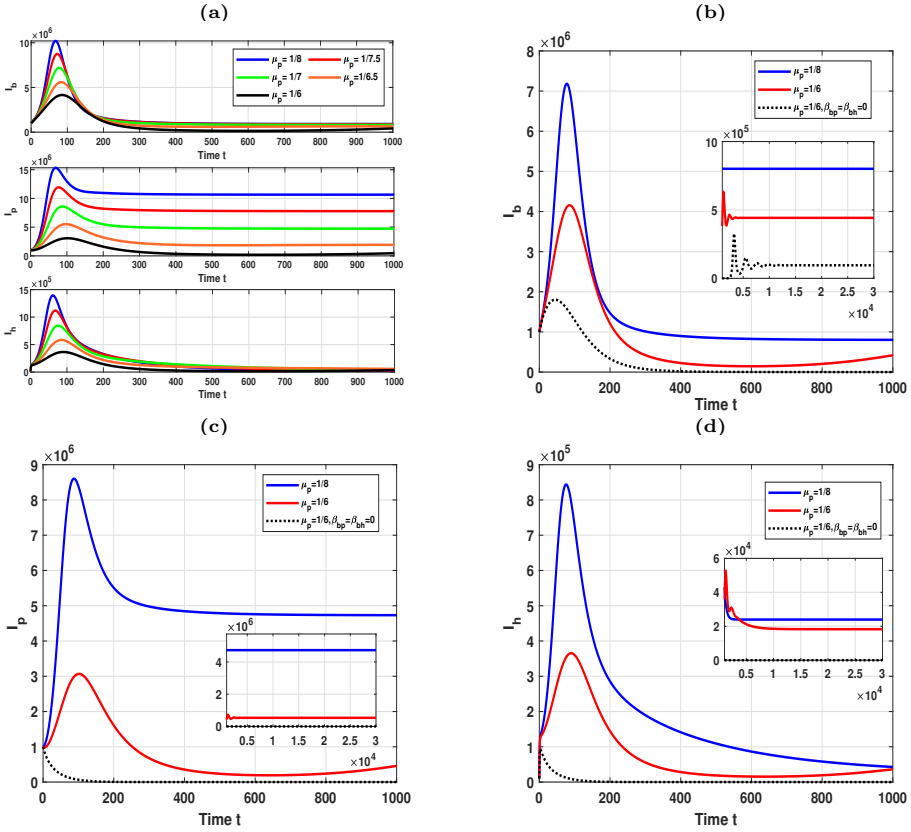

Figure 9. The impact of μ_p on the solutions related to infected population for model (2.1)

In addition, keeping the other parameters in Example 2 unchanged, we take three cases for the values of μ_p, β_{bp} and β_{bh}, and then calculate corresponding values of R_0^b, R_0^p and R_0 and get the final state values for infected patients, infected birds, and infected poultry(see Table 4). At the same time, the evolution solutions of system (2.1) for infected patients, infected birds, and infected poultry are respectively obtained (see Figs.9(b)-(d)). Similar to the arguments in Table 4, contrasting Case I and Case II in Table 4, we can also obtain that $R_0^b > 1$, $R_0^p > 1$, and $R_0 > 1$ change to $R_0^b > 1$, $R_0^p < 1$, and $R_0 > 1$ and the final size of infected birds, infected poultry and infected human has decreased, which means that the increase of the death rate μ_p can effectively reduce the final scale of the epidemic outbreak but can not control the disease transmission even if the $R_0^p < 1$. Moreover, contrasting Case

Table 4. Three cases to indicate the influence of μ_p on disease dynamics

Case	μ_p	β_{bp}	β_{bh}	R_0^b	R_0^p	R_0	$I_b(\infty)$	$I_p(\infty)$	$I_h(\infty)$
I	1/8	6.3243×10^{-10}	2.6245×10^{-10}	1.0994	1.3115	1.5554	800685	4729770	23966.9
II	1/6	6.3243×10^{-10}	2.6245×10^{-10}	1.0994	0.8918	1.2896	442119	535182	18282.9
III	1/6	0	0	1.0994	0.8918	1.0994	95548.8	0	0

II and Case III in Table 4, even though the basic reproduction numbers $R_0^b > 1$, $R_0^p < 1$, and $R_0 > 1$ unchanged, the final scale of the infected scale of infected poultry and infected humans comes to zero. Biologically, keeping the same death rate μ_p and cutting off the transmission from birds to poultry and humans($\beta_{bp} = \beta_{bh} = 0$) can make the final scale of the infected poultry and infected humans zero even if the basic reproduction numbers $R_0^b > 1$, $R_0^p < 1$, and $R_0 > 1$. Furthermore, we

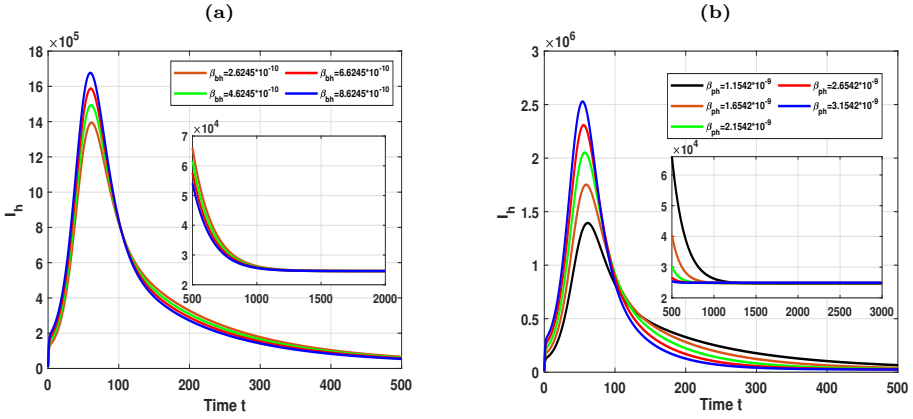

Figure 10. The impact of β_{bh} and β_{ph} on the solutions I_h for model (2.1)

investigate the influence of the transmission rate β_{bh} and β_{ph} on disease dynamics. In fact, the expression of basic reproduction number R_0 does not conclude β_{bh} and β_{ph}, which means that the values of β_{bh} and β_{ph} can not change the threshold dynamics. However, based on the sixth equation of system (2.1), it is not hard to find that their values will affect the scale of the number of infected humans. In order to visualize this phenomenon, we take different values of β_{bh} and keep the other parameters the same as Example 2. We get the evolution solutions of I_h (see Fig.10(a)), which shows that the peak values of infected humans will increase with the increase of β_{bh}. And then we take different values of β_{ph} and keep the other parameters the same as Example 2. We get the evolution solutions of I_h (see Fig.10(b)), which shows that the peak values of infected humans will increase with the increase of β_{ph}. Hence, we can conclude that enhancing public awareness of prevention, such as wearing protective clothing, can reduce the transmission from birds and poultry to humans, thereby reduce the scale of disease incidence.

7. Conclusion and discussion

This work focuses on AV transmission dynamics model with high coupled transmission routes among wild birds, poultry and humans. Our proposed model stems form the actual biological background and has strong practical biological significance but it poses great challenges to qualitative and quantitative analysis, especially the existence of an endemic equilibrium and its global asymptotic stability. Firstly, the threshold dynamics of three sub-models: (the bird-only model, poultry-only model and bird-poultry model in terms of the corresponding basic reproduction numbers are discussed in detail. Here, we use a lot of mathematical analysis techniques and

Graphic analysis with Matlab to study the bird-poultry model. Then, we discuss the threshold dynamics criteria for the whole model. Furthermore, the sensitivity of some parameters in model (2.1) to the basic reproduction number R_0 is conducted. Based on the results of sensitivity analysis, an optimal control problem is proposed, and finally the theoretical results are verified and the effects of some parameters on dynamics are visualized through numerical simulation. The visualization results of the numerical simulation reveal many important and practical conclusions: reducing the reproductive rate and increasing the mortality rate of poultry, can only control the disease by simultaneously cutting off the transmission from birds to poultry and humans even if the ultimate scale of the disease can be effectively controlled. In addition, enhancing public awareness of prevention to reduce the transmission from bird and poultry to humans is also effective in controlling the final scale of disease.

On the other hand, there are a lot of significant topics that deserve further consideration other than the open problems proposed in this manuscript. For instance, in this paper, we assume that the population is homogeneous. It may be more practical to consider the effects of spatial heterogeneity and white noise on the dynamics of AI. To the best of our knowledge, there is little literature studying the dynamics of reaction-diffusion AI with white noise because the Itô's formula is not applicable for mild solutions. In the future, we will develop research methods to solve such problems.

Acknowledgements

The authors of this paper are very thankful to anonymous reviewers and editors for their suggestions to improve the presentation of this paper.

References

[1] D. J. Alexander, *An overview of the epidemiology of avian influenza*, Vaccine, 2007, 25(30), 5637-5644.

[2] P.K.S. Chan, *Outbreak of Avian Influenza A(H5N1) Virus Infection in Hong Kong in 1997*, Clinical Infectious Diseases, 2022, Supplement_2(34), S58-S64.

[3] https://www.who.int/publications/m/item/cumulative-number-of-confirmed-human-cases-for-avian-influenza-a(h5n1)-reported-to-who--2003-2023--3-october-2023.

[4] https://www.who.int/teams/global-influenza-programme/avian-influenza/monthly-risk-assessment-summary.

[5] Y. Chen, Z. Jin, J. Zhang, Y. Wang and J. Zhang, *Global dynamical analysis of H5 subtype avian influenza model*, International Journal of Biomathematics 2022,(15)8, 2250058.

[6] S. Liu, L. Pang, S. Ruan and X. Zhang, *Global Dynamics of Avian Influenza Epidemic Models with Psychological Effect*, Computational and Mathematical Methods in Medicine, 2015, 913726.

[7] R.M. Anderson and R.M. May, *Infectious Diseases of Humans: Dynamics and Control*, Oxford University Press, Oxford, UK, 1991.

[8] M.J. Keeling and P. Rohani, *Modeling Infectious Diseases in Humans and Animals*, Princeton University Press, Princeton, NJ, USA, 2008.

[9] B. Zhou, D. Jiang, Y. Dai and T. Hayat, *Threshold dynamics and probability density function of a stochastic avian influenza epidemic model with nonlinear incidence rate and psychological effect*, Journal of Nonlinear Science, 2023, 33, 29.

[10] Y. Luo, T. Zheng, Z. Teng and L. Zhang, *Dynamics of a periodic stage-structure competitive model with two maturation delays*, Applied and Computational Mathematics, 2023, 22, 149-171.

[11] K. Ren, Q. Zhang, T. Li and T. Kang, *Stability analysis and optimal control of avian influenza model on complex networks*, Mathematical Methods in the Applied Sciences, 2021, 44, 9582-9599.

[12] T. Calvin, T. Berge and A.F. Feukouo, *Avian-human influenza epidemic model with diffusion, nonlocal delay and spatial homogeneous environment*, Nonlinear Analysis-Real World Applications, 2022, 67, 103615.

[13] L. Yang, D. Song, M. Fan and L. Gao, *Transmission dynamics and optimal control of H7N9 in China*, International Journal of Biomathematics, 2022, 15, 2250007.

[14] T. Zheng, L. Nie, H. Zhu, Y. Luo and Z. Teng, *Role of seasonality and spatial heterogeneous in the transmission dynamics of avian influenza*, Nonlinear Analysis-Real World Applications, 2022, 67, 103567.

[15] T. Kang and Q. Zhang, *Dynamics of a stochastic delayed avian influenza model with mutation and temporary immunity*, International Journal of Biomathematics, 2021, 14(5), 2150029.

[16] X. Yu and Y. Ma, *An avian influenza model with nonlinear incidence and recovery rates in deterministic and stochastic environments*, Nonlinear Dynamics, 2022, 108, 4611-4628.

[17] M.A. Mata, P. Greenwood and R. Tyson, *The relative contribution of direct and environmental transmission routes in stochastic avian flu epidemic recurrence: an approximate analysis*, Bulletin of Mathematical Biology, 2019, 81, 4484-4517.

[18] X. Zhang, *Global dynamics of a stochastic avian-human influenza epidemic model with logistic growth for avian population*, Nonlinear Dynamics, 2017, 90, 2331-2343.

[19] S. Liu, S. Ruan and X. Zhang, *Nonlinear dynamics of avian influenza epidemic models*, Mathematical Biosciences, 2017, 283, 118-135.

[20] L. Bourouiba, S.A. Gourley, R. Liu and J. Wu, *The interaction of migratory birds and domestic poultry and its role in sustaining avian influenza*, SIAM Journal on Applied Mathematics, 2011, 2(71), 487-516.

[21] J. Zhang, X. Ma and Z. Jin, *Stability analysis of an HIV/ AIDS epidemic model with sexual transmission in a patchy environment*, Journal of Biological Dynamics, 2023, 17(1), 2227216.

[22] Y. Luo, S. Tang, Z. Teng and L. Zhang, *Global dynamics in a reaction-diffusion multi-group SIR epidemic model with nonlinear incidence*, Nonlinear Analysis-Real World Applications, 2019, 50, 365-385.

[23] Y. Luo, L. Zhang, Z. Teng and T. Zheng, *Analysis of a general multi-group reaction-diffusion epidemic model with nonlinear incidence and temporary acquired immunity*, Mathematics and Computers in Simulation, 2021, 182, 428-455.

[24] T. Gard, *Persistence in stochastic food web models*, Bulletin of Mathematical Biology, 1984, 46, 357-370.

[25] X. Mao, *Stochastic Differential Equations and Applications*, Chichester: Horwood Publishing Limited, 2007.

[26] T. Zheng, L. Nie, Z. Teng, Y. Luo and S. Wang, *Analysis of an age-structured dengue model with multiple strains and cross immunity*, Electronic Journal of Qualitative Theory of Differential Equations, 2021, 50, 1-30.

[27] T. Zheng and L. Nie, *Modelling the transmission dynamics of two-strain Dengue in the presence awareness and vector control*, Journal of Theoretical Biology, 2018, 443, 82-91.

[28] P. Driessche and J. Watmough, *Reproduction numbers and sub-threshold endemic equilibria for compartmental models of disease transmission*, Mathematical Biosciences, 2002, 180, 29-48.

[29] J.K. Hale and S.M. Verduyn, *Introduction to Functional Differential Equations*, Springer-Verlag, New York, 1993.

[30] D.L. Lukes, *Differential Equations: Classical to Controlled*, Academic Press, vol.162, NY, USA, 1982.

[31] L.S. Pontryagin and V.G. Boltyanskii, *The Mathematical Theory of Optimal Processes*, American Control Conference 1987, 27 (3), 36-40.

[32] J. Zhang, Y. Li, Z. Jin and H. Zhu, *Dynamics analysis of an avian influenza a (H7N9) epidemic model with vaccination and seasonality*, Complexity, 2019, 4161287.